MOLECULAR AND CELLULAR BIOLOGY, Oct. 1995, p. 5777–5788 Vol. 15, No. 10
0270-7306/95/$04.00+0

mRNA Decay Mediated by Two Distinct AU-Rich Elements from c-*fos* and Granulocyte-Macrophage Colony-Stimulating Factor Transcripts: Different Deadenylation Kinetics and Uncoupling from Translation

CHYI-YING A. CHEN, NIANHUA XU, AND ANN-BIN SHYU*

Department of Biochemistry and Molecular Biology, Medical School, The University of Texas Houston Health Science Center, Houston, Texas 77030

Received 15 May 1995/Returned for modification 6 July 1995/Accepted 26 July 1995

Poly(A) tail removal is a critical first step in the decay pathway for many yeast and mammalian mRNAs. Poly(A) shortening rates can be regulated by *cis*-acting sequences within the transcribed portion of mRNA, which in turn control mRNA turnover rates. The AU-rich element (ARE), found in the 3′ untranslated regions of many highly labile mammalian mRNAs, is a well-established example of this type of control. It represents the most widespread RNA stability determinant among those characterized in mammalian cells. Here, we report that two structurally different AREs, the c-*fos* ARE and the granulocyte-macrophage colony-stimulating factor (GM-CSF) ARE, both direct rapid deadenylation as the first step in mRNA degradation, but by different kinetics. For c-*fos*-ARE-mediated decay, the mRNA population undergoes synchronous poly(A) shortening and is deadenylated at the same rate, implying the action of distributive or nonprocessive ribonucleolytic digestion of poly(A) tails. In contrast, the population of granulocyte-macrophage colony-stimulating factor ARE-containing mRNAs is deadenylated asynchronously, with the formation of fully deadenylated intermediates, consistent with the action of processive ribonucleolytic digestion of poly(A) tails. An important general implication of this finding is that different RNA-destabilizing elements direct deadenylation either by modulating the processivity at which a single RNase functions or by recruiting kinetically distinct RNases. We have also employed targeted inhibition of translation initiation to demonstrate that the RNA-destabilizing function of both AREs can be uncoupled from translation by ribosomes. In addition, a blockade of ongoing transcription has been used to further probe the functional similarities and distinctions of these two AREs. Our data suggest that the two AREs are targets of two distinct mRNA decay pathways. A general model for ARE-mediated mRNA degradation involving a potential role for certain heterogeneous nuclear ribonucleoproteins and ARE-binding proteins is proposed.

In recent years, the biological significance of the control of mRNA turnover as an important mechanism for the regulation of gene expression has been recognized (for reviews, see references 2, 18, and 19). The AU-rich element (ARE) found in the 3′ untranslated regions (UTRs) of many labile mRNAs represents the most common RNA stability determinant in mammalian cells. Its presence in the 3′ UTRs of a wide variety of mRNAs, such as cytokine, proto-oncogene, and many nuclear transcription factor mRNAs (6, 8, 23), suggests a critical role for the ARE in the regulation of gene expression during cell growth and differentiation.

Previously, we have suggested that AREs can be divided into two groups, AUUUA-containing and non-AUUUA-containing AREs (8). AUUUA-containing AREs can be further divided into two classes according to some other discernible sequence differences. One class, represented by the c-*fos* ARE, contains a few copies of scattered AUUUA motifs coupled with nearby uridylate-rich sequences. The other class, represented by the granulocyte-macrophage colony-stimulating factor (GM-CSF) ARE, tends to have multiple reiterations of the AUUU tetranucleotide which give rise to at least two overlapping copies of UUAUUUAUU nonamers (14, 29) and contribute to a generally high uridylate content. However, it has never been clearly established whether these two AREs mediate mRNA decay through distinct decay pathways. Moreover, although the destabilizing function of the GM-CSF ARE was the first to be demonstrated (23), its decay kinetics have never been addressed. Specifically, we have shown that the c-*fos* ARE directs mRNA decay through biphasic decay kinetics, rapid and synchronous poly(A) shortening followed by rapid decay of the RNA body (7, 25). Does GM-CSF-ARE-mediated mRNA decay follow the same kinetics as c-*fos*-ARE-mediated mRNA decay?

Several lines of evidence suggest that the two classes of AUUUA-containing AREs function by somewhat different mechanisms and that their destabilizing functions are differentially regulated. First, Schuler and Cole (22) reported that in a monocytic tumor cell line, the c-*fos* and c-*myc* 3′ UTRs bearing the AREs destabilized *neo* reporter mRNA, whereas the GM-CSF 3′ UTR also carrying an ARE did not. A similar discrimination between the two types of AREs has also been observed in nontransformed T cells. Lindsten et al. (15) showed that stimulation of quiescent primary T cells with antibodies against CD3/CD28 receptors specifically stabilized the mRNAs of four lymphokines, including GM-CSF mRNA, while c-*fos* and c-*myc* mRNAs remained labile in the same cells. They suggested that differences in the structures of the two types of AREs are important in conferring differential stability.

A second fundamental yet controversial issue is whether ARE-directed mRNA decay is coupled to protein translation and if so, by what mechanism. Koeller et al. (12) reported that the ability of the c-*fos* ARE to destabilize a heterologous mRNA is not dependent on ongoing translation of the message. In contrast, two other studies suggested that mRNA

* Corresponding author. Phone: (713) 792-5398. Fax: (713) 794-4150. Electronic mail address: abshyu@utmmg.med.uth.tmc.edu.

decay directed by the GM-CSF ARE is coupled to translation. Savant-Bhonsale and Cleveland (20) reported that the blockage of translation by a mutation of the ATG initiation codon to a TAG stop codon results in an increase in the steady-state level of the message containing the GM-CSF ARE compared with that of the fully translated wild-type mRNA. Aharon and Schneider (1) reported that translation restoration by inserting an internal ribosomal entry site into the mRNA 5′ UTR leads to specific destabilization of the corresponding mRNA which harbors a copy of the GM-CSF ARE in its 3′ UTR. While these studies suggest a different requirement for translational coupling between the two AREs, since different cell types, reporter mRNAs, and experimental conditions were used in each case, it is not yet clear whether under the same genetic background and physiological state the two AREs still exhibit the observed difference in translation dependency of their RNA-destabilizing functions.

Finally, two seemingly contradictory observations suggest that the two types of AREs display different sensitivities to two commonly used transcription inhibitors, actinomycin D (ActD) and 5,6-dichloro-1-β-D-ribofuranosyl-benzimidazole (DRB). Previously, we have shown that rapid mRNA decay mediated by the c-*fos* 3′ UTR bearing an ARE can be specifically impaired by treating cells with ActD or DRB (26), indicating that the destabilizing function of the c-*fos* ARE is sensitive to these inhibitors. In a separate study, Shaw and Kamen (23) reported that rapid decay of β-globin mRNA carrying the GM-CSF ARE in its 3′ UTR occurred following transcription inhibition by ActD treatment. These results suggested that ActD and DRB are useful tools for distinguishing between the possible functional differences of these two AREs.

In this report, we compare several critical properties of these two AREs with respect to their RNA-destabilizing functions under the same genetic background and experimental conditions. Our results provide several novel findings. First, the two AREs exhibit very different mRNA deadenylation kinetics. The c-*fos* ARE directs rapid and synchronous shortening of the poly(A) tail, which is indicative of distributive action of the RNase for degrading poly(A) tails. In contrast, GM-CSF-ARE-directed decay displays an asynchronous pattern of poly(A) shortening, which is characteristic of processive action of the RNase for poly(A) removal. These findings may have general and novel implications for the regulation of cytoplasmic deadenylation that serves as a critical first step in the decay of many mRNAs in yeast and mammalian cells (for a review, see reference 2). Second, targeted inhibition of translation initiation by hairpin insertion has little effect on the destabilizing ability of either ARE, demonstrating that decay directed by these two AREs can be uncoupled from ongoing translation. Finally, two commonly used transcription inhibitors, ActD and DRB, have distinctly different impeding effects on mRNA decay mediated by these two AREs. This observation also suggests a role for ongoing transcription as well as certain heterogeneous nuclear ribonucleoproteins (hnRNP) and ARE-binding proteins in ARE-mediated mRNA decay.

MATERIALS AND METHODS

Plasmid constructions. When necessary, DNA with 5′ or 3′ protruding ends was treated with Klenow fragment or T4 DNA polymerase to make the ends blunt. The construction of plasmids pBBB, pBFB, and pBBB+ARE$^{c\text{-}fos}$ has been described previously (26). To construct pBBB+ARE$^{GM\text{-}CSF}$, a 163-bp *Eco*RI-*Bgl*II fragment containing the last 80 bp of the carboxyl-terminal region of the rabbit β-globin gene and the GM-CSF AT sequences (23) immediately downstream of it was amplified by standard PCR techniques with plasmid β-globin^{AT} (23) as the template. After *Eco*RI and *Bgl*II digestion, the PCR fragment was subcloned between the *Eco*RI and *Bgl*II sites of plasmid pBBB. To introduce the hairpin into the 5′ UTRs of β-globin messages and its derivatives, a *Bsa*BI site 20 bp downstream of the transcription initiation site of the β-globin gene was created by recombinant PCR mutagenesis (10). A 48-bp DNA fragment encoding the desired hairpin (Fig. 1) was then prepared by *Hin*dIII and *Bam*HI digestions of plasmid SP64-hp7 (13), which was kindly provided by Marilyn Kozak, blunt ended, and inserted into the *Bsa*BI sites of pBBB, pBFB, pBBB+ARE$^{c\text{-}fos}$, and pBBB+ARE$^{GM\text{-}CSF}$ to generate pBBB-hp, pBFB-hp, BBB+ARE$^{c\text{-}fos}$-hp, and BBB+ARE$^{GM\text{-}CSF}$-hp, respectively.

Cell culture and DNA transfection. Culture, transient transfection, and serum stimulation of mouse NIH 3T3 cells were performed as described previously (26). ActD and DRB were purchased from Sigma Chemical Co.

Analysis of mRNA decay and deadenylation. Total cytoplasmic RNA was isolated at various times after serum stimulation of transiently transfected NIH 3T3 cells, and mRNA decay and deadenylation were analyzed by Northern (RNA) blot analysis as described previously (25). To analyze mRNA decay, α-glyceraldehyde-3-phosphate dehydrogenase (α/GAPDH) mRNA (8) was used in transient transfection experiments as an internal control and standard. Electrophoresis was done on 1.4% formaldehyde agarose gels. A 123-nucleotide (nt) single-stranded DNA ladder (Bethesda Research Laboratories [BRL]) was included to provide a molecular size standard. Gene-specific DNA probes were prepared by random oligonucleotide priming. Labeled probes were produced by the inclusion of [α-^{32}P]dCTP (>6,000 Ci/mmol; Amersham). RNase H treatment of cytoplasmic mRNA was carried out as described previously (25). mRNA decay was quantitated directly by scanning blots on a Betascope 603 blot analyzer (Betagen).

Polysome profile analysis. Approximately 5×10^7 cells transiently cotransfected with the constructs of interest were serum starved for 25 h and then serum induced for 30 min; from these cells, cytoplasmic lysates were prepared with 1 ml of ice-cold lysis buffer (50 mM Tris-HCl [pH 8.0], 100 mM NaCl, 5 mM $MgCl_2$, 0.5% Nonidet P-40, 200 U of RNasin per ml). After centrifugation (10,000 × *g* to 15,000 × *g*) at 4°C, each supernatant was mixed with 6.7 μl of heparin (100 mg/ml), 15 μl of cycloheximide (10 mg/ml), 20 μl of dithiothreitol (1 M), and 10 μl of phenylmethylsulfonyl fluoride (0.1 M) and was layered on a continuous sucrose gradient (15 to 40% RNase-free sucrose in 10 mM Tris-HCl [pH 7.5]–140 mM NaCl–1.5 mM $MgCl_2$). Gradients were centrifuged at 38,000 rpm for 2 h at 4°C in a Beckman SW41 rotor. Twenty fractions were collected, and RNA was extracted from each fraction as previously described (25). RNA samples were analyzed by 1% agarose gel electrophoresis to resolve the polysome profile for each fractionation. Further analyses of the specific distribution of tested mRNAs and the control α/GAPDH mRNA in these fractions were done by Northern blotting as described above.

RESULTS

Patterns of rapid mRNA decay mediated by the c-*fos* and GM-CSF AREs display different deadenylation kinetics. Although the ability of the GM-CSF ARE to destabilize a heterologous stable mRNA was the first to be demonstrated (23), the precise decay kinetics of GM-CSF-ARE-directed mRNA decay have never been described. To define the kinetic characteristics of GM-CSF-ARE-mediated mRNA decay under conditions which would permit direct comparison with those of c-*fos*-ARE-mediated mRNA decay, the human GM-CSF ARE was subcloned into a unique *Bgl*II site in the 3′ UTR of the rabbit β-globin gene, whose transcription is driven by the serum-inducible c-*fos* promoter (Fig. 1). The β-globin gene containing either of these AREs in its 3′ UTR (BBB+ARE) was introduced into NIH 3T3 cells by transient cotransfection with a control gene. The control mRNA (α/GAPDH mRNA), which was expressed in a constitutive way, served as an internal control for correcting variations in transfection efficiency and sample handling. Transcription from BBB+ARE genes and their derivatives were then transiently induced by stimulation with 20% calf serum. Total cytoplasmic mRNA was isolated at time intervals and analyzed by Northern blotting.

As expected from our previous studies (7, 25), β-globin mRNA containing the c-*fos* ARE underwent rapid decay with a biphasic pattern (Fig. 2). During the first phase, the poly(A) tails of the BBB+ARE$^{c\text{-}fos}$ mRNA population underwent synchronous and rapid deadenylation to a size of 30 to 60 nt while the mRNA concentration remained fairly constant. In the second phase, the transcribed portion of the mRNA or the mRNA body was degraded with apparent first-order kinetics.

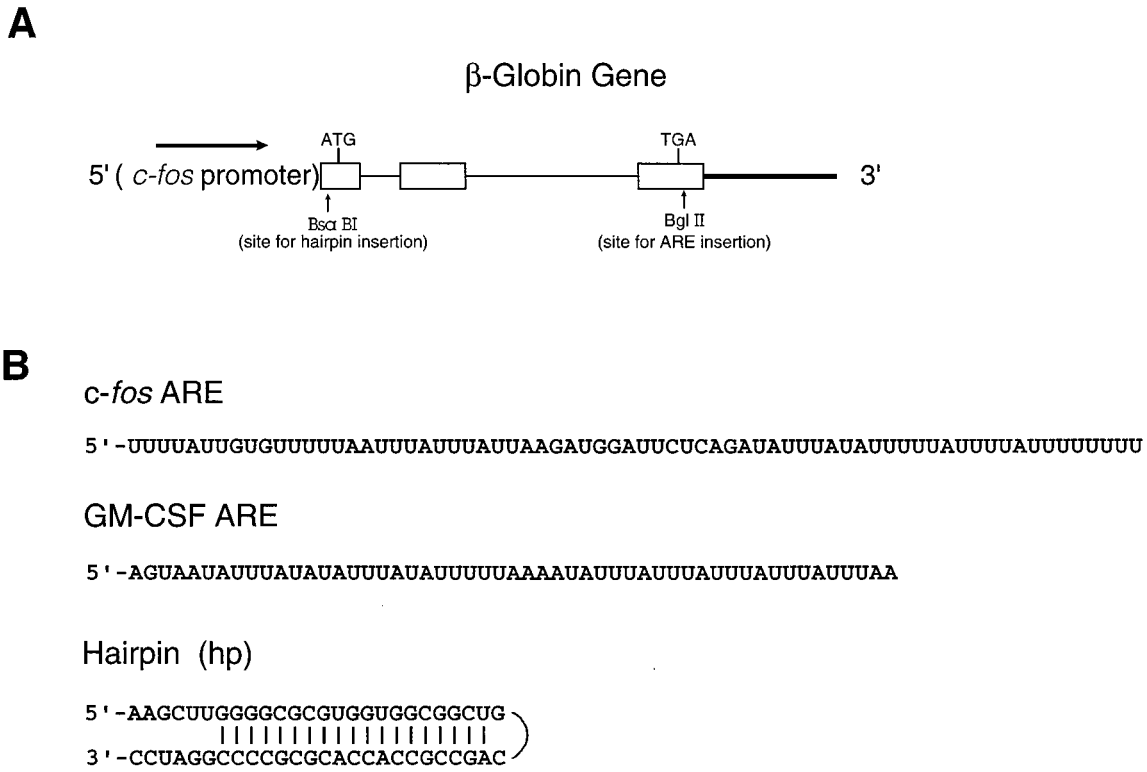

FIG. 1. (A) Physical map of the β-globin gene, whose transcription is driven by the serum-inducible c-*fos* promoter. The sequences encoding the translation initiation codon (ATG) and the termination codon (TGA), a unique *Bgl*II site for ARE insertion, and a *Bsa*BI site, which was created by site-directed mutagenesis for the hairpin insertion, are indicated. (B) RNA sequences of the c-*fos* ARE, GM-CSF ARE, and hairpin. Potential base pairing of the hairpin is indicated by connecting each pair with a line as indicated.

The fairly synchronous and universal shortening of poly(A) tails suggested that this step was catalyzed by a nonprocessive or distributive RNase. In contrast, GM-CSF-ARE-directed mRNA decay exhibited very different decay kinetics. Beginning at the 45-min time point when transcription of the c-*fos* promoter was already shut off, the major population of BBB+ARE$^{GM\text{-}CSF}$ mRNA underwent immediate and rapid decay (Fig. 2). There was no apparent time lag for the decay of this major population of BBB+ARE$^{GM\text{-}CSF}$ mRNA. While the major population of BBB+ARE$^{GM\text{-}CSF}$ mRNA was quickly degraded with first-order kinetics (Fig. 2A and 3 [open triangles]), a minor band corresponding to the poly(A)$^-$ species appeared simultaneously with the commencement of RNA decay at 45 min and persisted with slightly increasing intensity until the 120-min time point when decay of the major population of mRNA was nearly completed (Fig. 2A and 3 [filled triangles]). Further treatment of RNA samples from 30- to 90-min time points with RNase H and oligo(dT) demonstrated that the minor band is a poly(A)$^-$ species (Fig. 3). These results are consistent with the interpretation of a precursor-product relationship between the major population of poly(A)$^+$ RNA (Fig. 3 [open triangles]) and the minor poly(A)$^-$ band (Fig. 3 [filled triangles]). The low abundance of the poly(A)$^-$ RNA species suggests that after its formation, the poly(A)$^-$ RNA is quickly degraded. The data further suggest that before the mRNA containing the GM-CSF ARE can be degraded, its poly(A) tail has to be removed by an RNase characterized by a fairly processive action. Taken together, the observed kinetic characteristics and intermediates are indicative of a rather nonprocessive enzymatic action for c-*fos*-ARE-mediated poly(A) shortening and a fairly processive enzymatic action for GM-CSF-ARE-directed deadenylation (see Discussion). Therefore, we conclude that while rapid deadenylation is a prerequisite for both c-fos-ARE- and GM-CSF-ARE-mediated mRNA decay, mRNA decay directed by these two AREs exhibits kinetically distinct deadenylation reactions.

The RNA-destabilizing functions of these two AREs can be uncoupled from ongoing translation by ribosomes in NIH 3T3 cells. We next addressed whether the destabilizing functions of these two structurally distinct AREs have to be coupled to protein translation by ribosomes. To test this point, we utilized targeted inhibition of translation initiation by hairpin insertions at the 5′ UTRs of mRNAs. The advantage of this approach is that the translation-inhibitory effect is specific for mRNA bearing the hairpin. Moreover, inhibition of global protein synthesis by translation inhibitors, e.g., cycloheximide (which causes a profound disturbance of cell physiology), is avoided. A 48-bp cDNA encoding a strong RNA hairpin was chosen (Fig. 1B) (13) because previously we had shown that the hairpin is capable of blocking translation initiation when it is inserted in the 5′ UTR of a labile c-*fos* mRNA derivative (FΔ4 mRNA) from which the ARE has been deleted (21). Therefore, its decay would be due to instability determinants in the c-*fos* protein coding region. In this example, hairpin insertion led to specific stabilization of the labile FΔ4 mRNA. Thus, to block translation initiation of β-globin mRNA carrying the c-*fos* ARE or the GM-CSF ARE, the hairpin DNA was introduced into the unique *Bsa*BI site which had been created in the 5′ UTR of the β-globin gene and was 20 nt downstream from transcription initiation site (Fig. 1A). The resulting mRNAs were termed BBB+ARE$^{c\text{-}fos}$-hp and BBB+ARE$^{GM\text{-}CSF}$-hp.

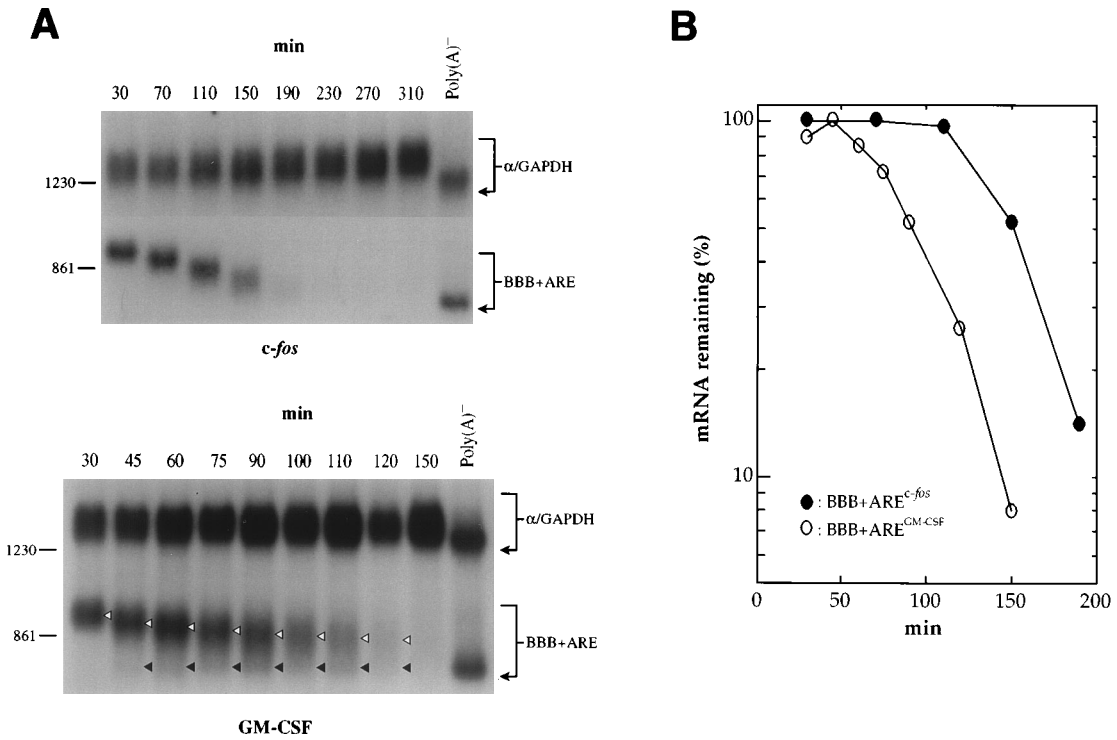

FIG. 2. β-Globin mRNAs carrying the c-*fos* ARE and those carrying the GM-CSF ARE decay with different kinetics. NIH 3T3 cells were transiently cotransfected with control plasmid pSVα1/GAPDH and one of the test plasmids. Total cytoplasmic mRNA was isolated at various time intervals after serum stimulation and analyzed by Northern blot analysis. α/GAPDH mRNA was expressed constitutively and served as an internal standard for these experiments. (A) Northern blots showing the decay of BBB+ARE$^{c\text{-}fos}$ and BBB+ARE$^{GM\text{-}CSF}$ mRNAs. Note that the somewhat broad band corresponding to α/GAPDH mRNA in each blot is due to poly(A) tail heterogeneity caused by the constitutive transcription of the α/GAPDH gene and subsequent asynchronous poly(A) shortening of α/GAPDH mRNAs in the cytoplasm. The times given at the top correspond to minutes after serum stimulation. At 30 min after serum induction, BBB+ARE mRNA still retained a full-length poly(A) tail (~200 nt). Poly(A)$^-$ RNA was prepared in vitro by treating RNA samples from the 30-min time point with oligo(dT) and RNase H. The major and minor species of BBB+ARE$^{GM\text{-}CSF}$ mRNA are depicted by open and filled triangles, respectively. A 123-bp DNA ladder from BRL was used as the molecular size standard. The positions corresponding to 861 and 1,230 nt are indicated on the left. (B) Semilog plots showing the decay of BBB+ARE$^{c\text{-}fos}$ and BBB+ARE$^{GM\text{-}CSF}$ mRNAs. The quantitation of data was obtained by scanning the radioactive blots with a Betascope blot analyzer (Betagen).

To demonstrate the feasibility of the approach described above, the stabilization effect of hairpin insertion on the destabilizing function of determinants in the c-*fos* protein coding region was first determined by analyzing a control message, BFB-hp. BFB-hp mRNA serves as a better control for this study than FΔ4hp mRNA since the BFB-hp gene was constructed by inserting the hairpin into the same site in the β-globin 5′ UTR (Fig. 1) of a chimeric BFB gene which contains the β-globin 5′ and 3′ UTRs and the c-*fos* protein coding region. Previously, we have shown that BFB mRNA has a very short half-life (<20 min) and that its lability is due to the presence of the c-*fos* coding region determinants of instability (25, 26). As shown in Fig. 4 (top panel), while the endogenous c-*fos* mRNA remained unstable, BFB-hp mRNA became stable upon hairpin insertion. Its half-life increased from less than 20 min to more than 10 h. These data demonstrate that the hairpin insertion at the *Bsa*BI site in the β-globin 5′ UTR is indeed able to lead to BFB RNA stabilization.

Having demonstrated the feasibility of the hairpin insertion approach, we then examined the decay of BBB+ARE$^{c\text{-}fos}$-hp and BBB+ARE$^{GM\text{-}CSF}$-hp mRNAs. As shown in Fig. 5A, there was little change in the lability of either mRNA. To compare these results with those for experiments performed without hairpin insertions (Fig. 2), decay curves were plotted (Fig. 5B). It is clear from the semilog plots that the hairpin insertion in the 5′ UTR had very little effect on the destabilizing function of either ARE. It is worth noting that while the

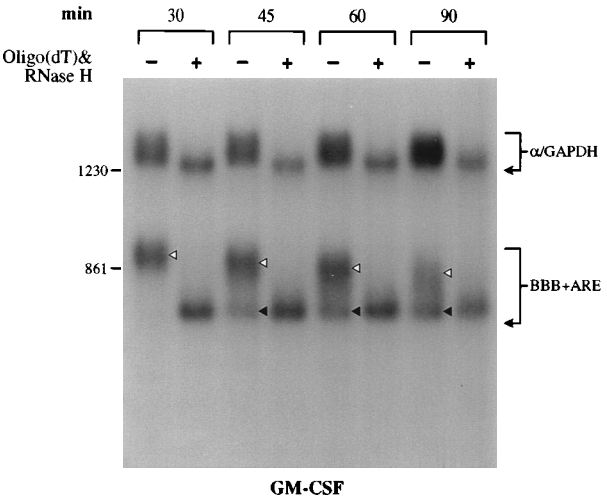

FIG. 3. The minor band appearing simultaneously with the commencement of decay of major BBB+ARE$^{GM\text{-}CSF}$ mRNA population is poly(A)$^-$ RNA. Transient transfection, RNA isolation, and time course experiments were carried out as described in the legend to Fig. 2. The times given at the top correspond to minutes after serum stimulation. The major and minor species of BBB+ARE$^{GM\text{-}CSF}$ mRNA are depicted by open and filled triangles, respectively. Poly(A)$^-$ RNA was prepared in vitro by treating the RNA sample from each time point with oligo(dT) and RNase H. A 123-bp DNA ladder from BRL was used as the molecular size standard. The positions corresponding to 861 and 1,230 nt are indicated on the left.

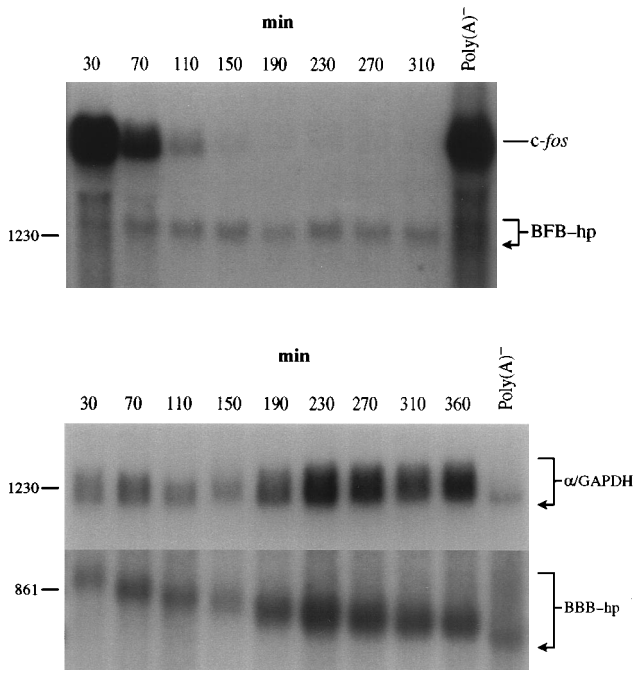

FIG. 4. Decay of BFB-hp and BBB-hp mRNAs showing the feasibility of the hairpin insertion approach. Transient transfection, RNA isolation, and time course experiments were carried out as described in the legend to Fig. 2. The times given at the top correspond to minutes after serum stimulation. Poly(A)$^-$ RNA was prepared in vitro by treating the RNA sample from each time point with oligo(dT) and RNase H. A 123-bp DNA ladder from BRL was used as the molecular size standard. The positions corresponding to 861 and 1,230 nt are indicated on the left.

hairpin insertion did not affect the deadenylation kinetics of the GM-CSF ARE, this manipulation significantly changed the deadenylation kinetics of the c-*fos* ARE; they were similar to those of the GM-CSF ARE (compare Fig. 2A and 5A; see Discussion).

To directly demonstrate that the hairpin insertion blocked translation initiation of the tested mRNAs, we performed polysome profile studies to critically evaluate the translation statuses of the following four mRNAs: BBB+ARE$^{c\text{-}fos}$, BBB+ARE$^{c\text{-}fos}$-hp, BBB+ARE$^{GM\text{-}CSF}$, and BBB+ARE$^{GM\text{-}CSF}$-hp. If the hairpin efficiently blocked translation initiation, the mRNA distribution was expected to shift from polysome fractions to nonpolysome fractions containing ribosomal subunits. As a control, the polysome profile of α/GAPDH mRNA, which did not carry the hairpin, was also determined in the same experiment. A typical example is shown in Fig. 6A. The ethidium bromide-stained gel revealed a well-resolved polysome profile for each fractionation, and fractions corresponding to the ribosome-free 40S, 60S, 80S, and polysomes were easily identified and displayed the characteristic features. Further analyses of the specific distribution of the BBB+ARE, BBB+ARE-hp, and control α/GAPDH mRNAs in these fractions by Northern blotting clearly showed that insertions of the hairpin into the BBB+ARE$^{c\text{-}fos}$ and BBB+ARE$^{GM\text{-}CSF}$ mRNAs changed the distribution of both messages from throughout the polysome fractions to fractions corresponding only to ribosome subunits (Fig. 6B and C). In contrast, the polysome profiles of control α/GAPDH messages remained unchanged in all experiments. Therefore, these results demonstrate an efficient blockade of translation initiation by hairpin insertion and strongly support translation-independent mRNA-destabilizing functions for these two AREs.

To rule out the possibility that the lability of BBB+ARE-hp messages was due to destabilization invoked by the insertion of the hairpin into the 5′ UTR of β-globin mRNA rather than destabilization mediated by AREs, transient transfection was carried out with control plasmid pBBB-hp. This plasmid contains the gene encoding wild-type β-globin mRNA with the hairpin insertion in its 5′ UTR at the same position as in the other ARE-containing constructs. As shown in Fig. 4 and 5B, the decay kinetics and stability of β-globin mRNA remained unchanged upon hairpin insertion into its 5′ UTR. Therefore, blockage of translation initiation by hairpin insertion in the β-globin 5′ UTR per se has no destabilizing effect. These results demonstrate that the RNA-destabilizing function of either ARE is not obligatorily coupled to translation by ribosomes.

Two commonly used transcription inhibitors, ActD and DRB, have specific inhibitory effects on the RNA-destabilizing functions of the c-*fos* and GM-CSF AREs. To test the possibility that ActD has a differential impeding effect on the RNA-destabilizing functions of these two AREs, BBB+ARE$^{c\text{-}fos}$ and BBB+ARE$^{GM\text{-}CSF}$ mRNAs were expressed upon serum induction of quiescent NIH 3T3 cells. ActD (5 μg/ml) was then added 25 min after serum induction, and mRNA decay of the two messages was determined as a function of time. Remarkably, as shown in Fig. 7A and B (top blots), ActD had a profound stabilization effect, completely blocking the decay of both mRNAs. Moreover, poly(A) shortening directed by either ARE was also significantly retarded. Interestingly, after transcription inhibition by ActD, the control α/GAPDH message, whose synthesis was driven by the simian virus 40 enhancer, decayed much faster than either ARE-containing mRNA. This was due to the inhibition of transcription from the simian virus 40 early promoter by ActD so that decay of α/GAPDH hybrid mRNA could be monitored. These results indicate that the inhibitory effect of ActD on the destabilizing functions of these two AREs is fairly specific.

To address more specifically which step of mRNA decay mediated by the c-fos ARE or the GM-CSF ARE was blocked by ActD, this inhibitor was also added to cells at later time points after serum induction (100 and 140 min for the c-*fos* ARE and 80 min for the GM-CSF ARE) in three separate time course experiments. As shown in the two lower blots of Fig. 7A, regardless of when this inhibitor was added, the decay of BBB+ARE$^{c\text{-}fos}$ mRNA was completely blocked in less than 10 min after the addition of ActD to cells. For example, when the drug was added at 110 min, a time immediately preceding the commencement of decay of the RNA body, subsequent RNA decay was blocked (Fig. 7A, middle blot). Similarly, when ActD was added at 140 min after serum induction, when the second step in the decay of the RNA body had just commenced, it completely blocked the second step and no subsequent decay of the RNA body was detected (Fig. 7A, bottom blot). These results clearly showed that even when the decay of the RNA body had commenced, ActD could still block any further proceeding of this step. Therefore, ActD is capable of blocking both steps of the two-phase decay mediated by the c-*fos* ARE. Interestingly, the addition of ActD at the 80-min time point has only a modest effect on the GM-CSF ARE (Fig. 7B, bottom blot). The subsequent decay of BBB+ARE$^{GM\text{-}CSF}$ mRNA was slightly retarded (Fig. 7B, bottom bot). Nevertheless, the rapid action of ActD suggests that its inhibition of ARE-mediated decay is the result of a relatively direct effect. These results also suggest that an ActD-sensitive or -inducible factor(s) is directly involved in RNA decay mediated by both AREs and that the factor(s) is involved in not only poly(A) shortening but also the decay of the RNA body.

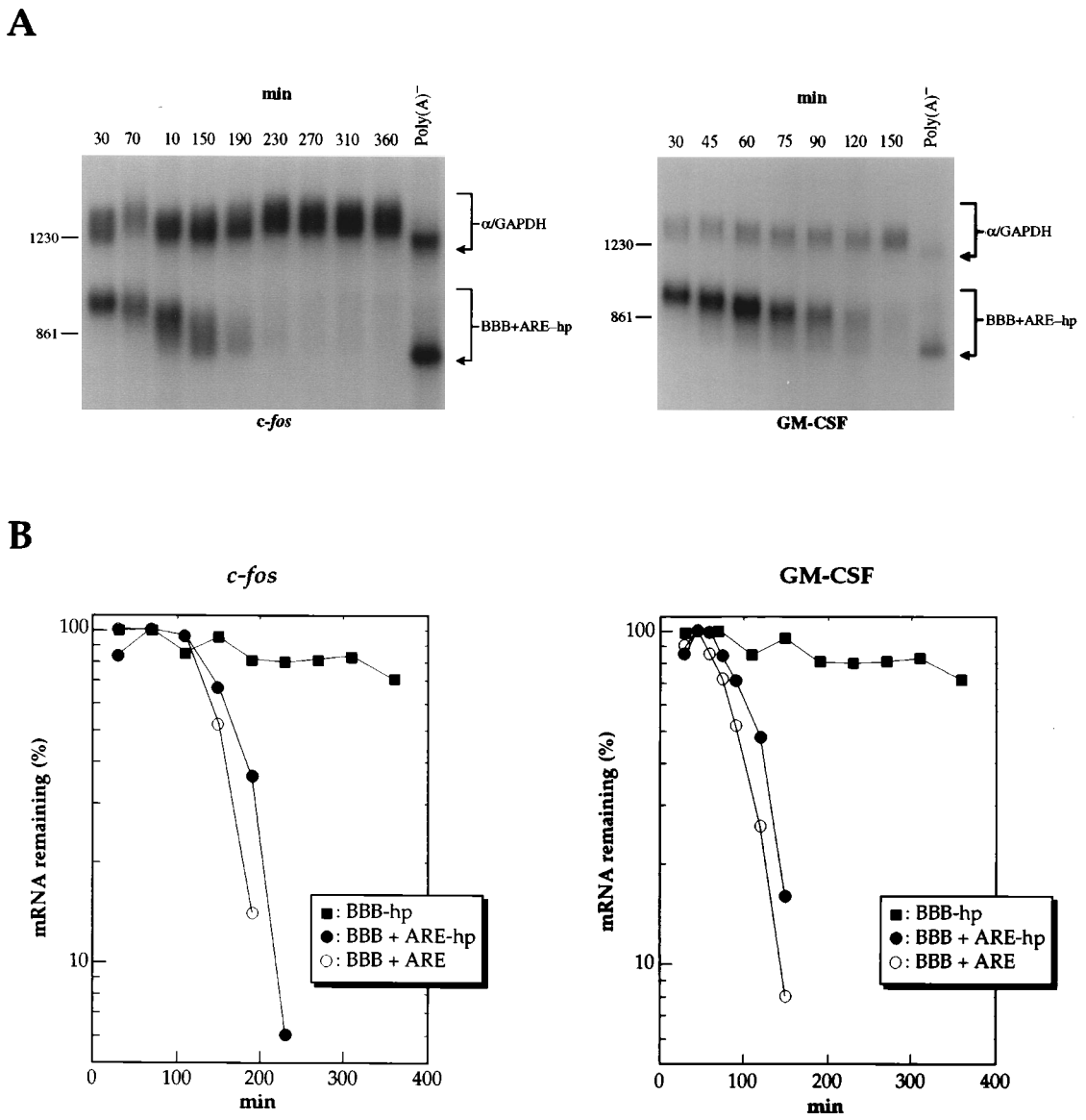

FIG. 5. RNA-destabilizing functions of the c-*fos* and GM-CSF AREs can be uncoupled from ongoing translation by ribosomes in NIH 3T3 cells. (A) Northern blots showing the decay of BBB+ARE$^{c\text{-}fos}$-hp mRNA and pBBB+ARE$^{GM\text{-}CSF}$-hp mRNA. Transient cotransfection of NIH 3T3 cells with control plasmid pSVα1/GAPDH and one of the test plasmids and subsequent analysis of mRNA decay were carried out as described in the legend to Fig. 2. The times given at the top correspond to minutes after serum stimulation. At 30 min after serum induction, BBB+ARE mRNA still retained a full-length poly(A) tail (~200 nt). Poly(A)$^-$ RNA was prepared in vitro by treating RNA samples from the 30-min time point with oligo(dT) and RNase H. A 123-bp DNA ladder from BRL was used as the molecular size standard. The positions corresponding to 861 and 1,230 nt are indicated on the left. (B) Semilog plots showing the decay of BBB+ARE, BBB+ARE-hp, and BBB-hp mRNAs. The quantitation of data was obtained by scanning the radioactive blots with a Betascope blot analyzer (Betagen).

To gain further insight into the decay-impeding effects of transcription inhibitors, a second transcription inhibitor, DRB, was used at a concentration of 20 μg/ml. We reasoned that if ActD had a direct effect on ARE-directed decay by, for instance, intercalating into the RNA secondary structure, which in turn could disrupt the RNA-protein complex formed on the ARE, DRB, a polymerase II-specific transcription inhibitor, should not display such an effect. As shown in Fig. 8, although less potent than ActD, DRB also exhibited a rapid and reproducible impeding effect on the destabilizing functions of both AREs, causing significant stabilization of the BBB+ARE$^{c\text{-}fos}$ mRNA and modest stabilization of the BBB+ARE$^{GM\text{-}CSF}$ mRNA. It significantly retarded poly(A) shortening directed by the c-*fos* ARE; therefore, the time lag before commencement of the decay of the RNA body increased significantly. The rapid decay of the RNA body of BBB+ARE$^{c\text{-}fos}$ mRNA starting at the 240-min time point was also slightly retarded. These results showed that two mechanistically distinct transcription inhibitors can have decay-impeding effects on ARE-mediated decay, albeit to different extents, suggesting the involvement of ongoing nuclear transcription in ARE-directed mRNA decay.

DISCUSSION

Despite numerous investigations of its mode of action, the mechanism and regulation of mRNA decay mediated by the ARE has remained poorly understood. A serious complication

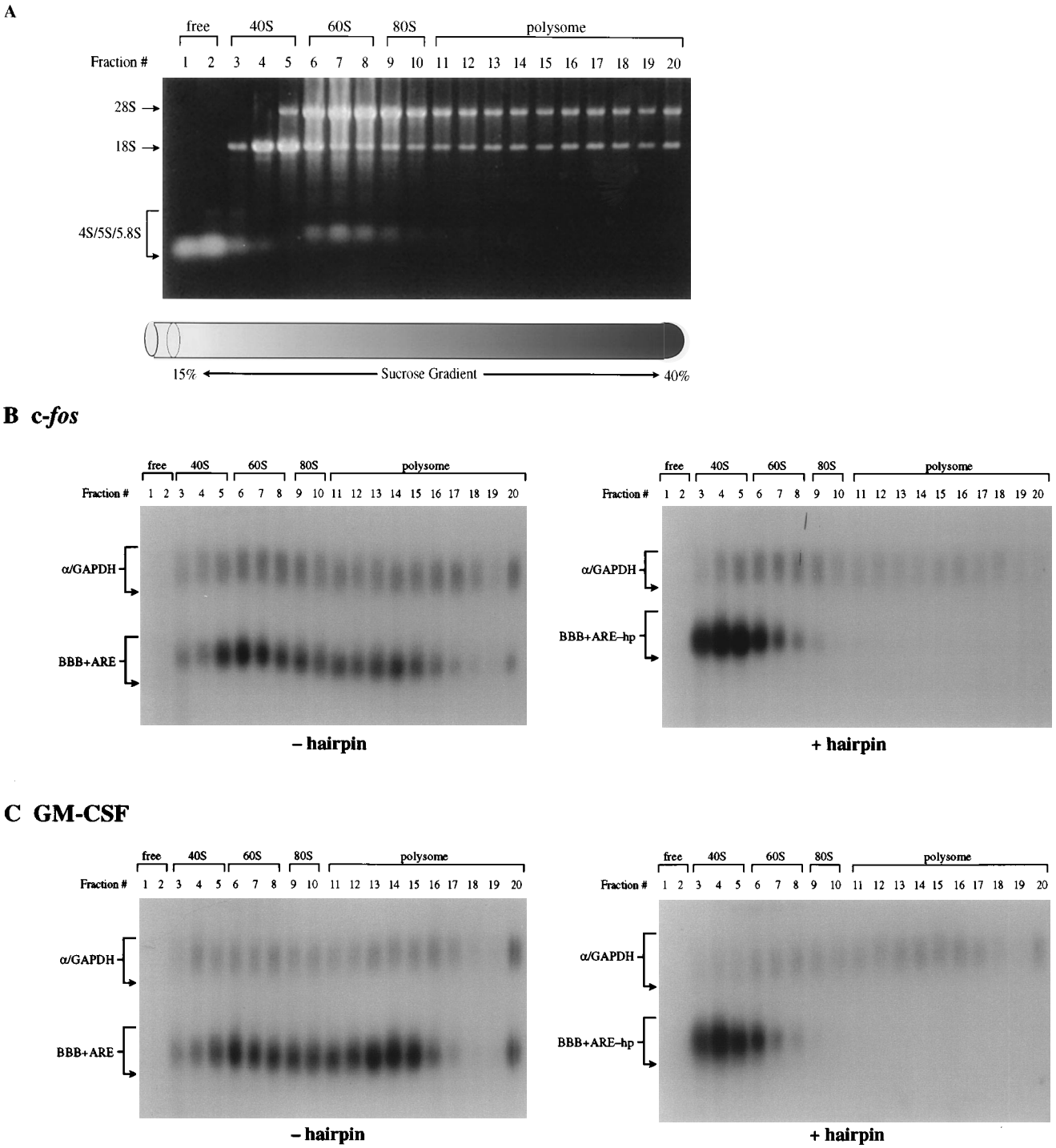

FIG. 6. Polysome profiles showing that hairpins inserted in the 5′ UTRs of BBB+ARE mRNAs efficiently and specifically blocked the ongoing translation of messages. (A) Typical polysome profile. Transient cotransfection of NIH 3T3 cells was carried out as described in the legend to Fig. 2. Cells transiently cotransfected with the corresponding constructs were serum starved for 25 h and then serum induced for 30 min. Cytoplasmic lysates were prepared and fractionated on a continuous sucrose gradient (15 to 40%) to resolve the ribosome subunits and polysomes (for details, see Materials and Methods). Polysome profiles were obtained by running RNA samples from each fraction on a 1% agarose gel, which was subsequently stained with ethidium bromide. The positions of the 40S, 60S, and 80S ribosomal subunits as well as polysomes are marked. (B) Distribution of BBB+ARE$^{c\text{-}fos}$ mRNA with (+) or without (−) the hairpin and of the internal control message (α/GAPDH mRNA) as identified by Northern blotting. (C) Distribution of BBB+ARE$^{GM\text{-}CSF}$ mRNA with or without the hairpin and of the internal control message (α/GAPDH mRNA) in the polysome profile as identified by Northern blotting.

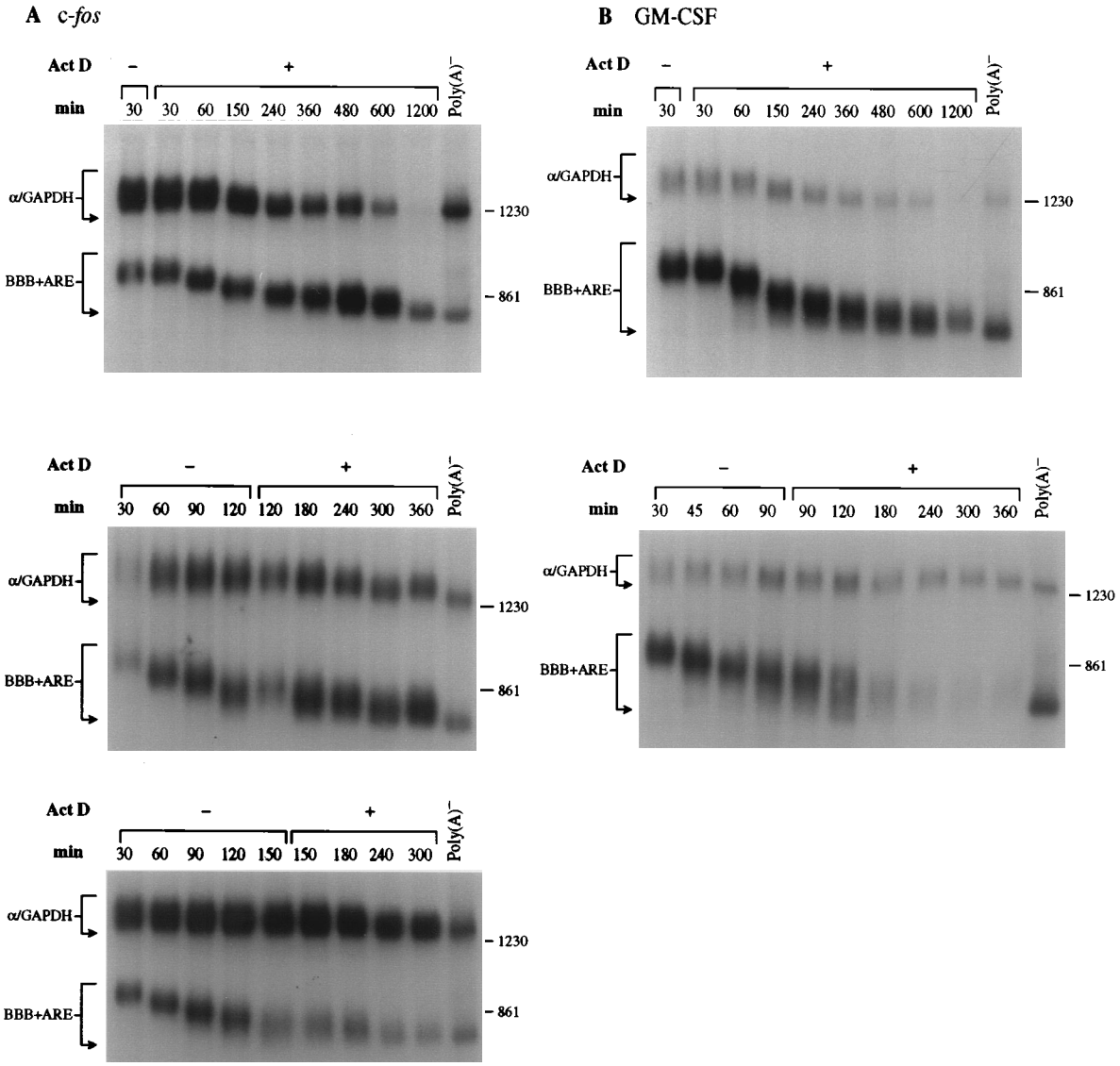

FIG. 7. Transcription inhibitor ActD selectively impeded the destabilizing functions of both c-*fos* and GM-CSF AREs. Transient cotransfection of NIH 3T3 cells with control plasmid pSVα1/GAPDH and test plasmid pBBB+ARE$^{c\text{-}fos}$ (A) or pBBB+ARE$^{GM\text{-}CSF}$ (B) and subsequent analysis of mRNA decay were carried out as described in the legend to Fig. 2. ActD (5 μg/ml) was added to the culture medium at 25 (panels A and B, top blots), 80 (panel B, bottom blot), 100 (panel A, middle blot), or 140 min (panel A, bottom blot) after serum induction. The times given above each blot correspond to minutes after serum stimulation when the RNA samples were extracted from cells with (+) or without (−) ActD treatment. Poly(A)$^-$ RNA was prepared in vitro by treating RNA samples from the 30-min time point with oligo(dT) and RNase H. A 123-bp DNA ladder from BRL was used as the molecular size standard. The positions corresponding to 861 and 1,230 nt are indicated on the right.

arises when published information from different experimental systems concerning how the destabilizing function of the c-*fos* ARE and the GM-CSF ARE may be regulated is compared. In this study, we have directly compared the effects of these critical factors on the destabilizing functions of these two classes of AREs. A critical and major difference between our investigation and previous studies is that in our study, the two AREs were introduced into the same reporter mRNA and their destabilizing functions were directly compared in the same genetic background and experimental conditions.

Several lines of evidence from our experiments argue that these two AREs mediate mRNA decay via distinct pathways that appear to use deadenylation as a critical first step. First, the apparent decay kinetics of these two AREs are different. The c-*fos* ARE directs a biphasic mRNA degradation, in which a time lag is followed by rapid decay of the RNA body with first-order kinetics (Fig. 2). In contrast, the decay directed by the GM-CSF ARE appears to commence immediately after the cessation of transcription between the 30- and 45-min time points (Fig. 2). Second, they exhibit very different deadenylation kinetics. The c-*fos* ARE directs rapid and synchronous poly(A) shortening, whereas the GM-CSF ARE induces asynchronous shortening of the poly(A) tail (Fig. 2A). These observations suggest that fundamental differences exist between these two AREs in terms of the composition of the decay complex formed on each ARE in cells and as to how the complex influences poly(A) removal activity and subsequent decay of the RNA body (see below). Third, although the destabilizing functions of these two AREs are not affected by the translation status of the mRNA bearing them, an obvious al-

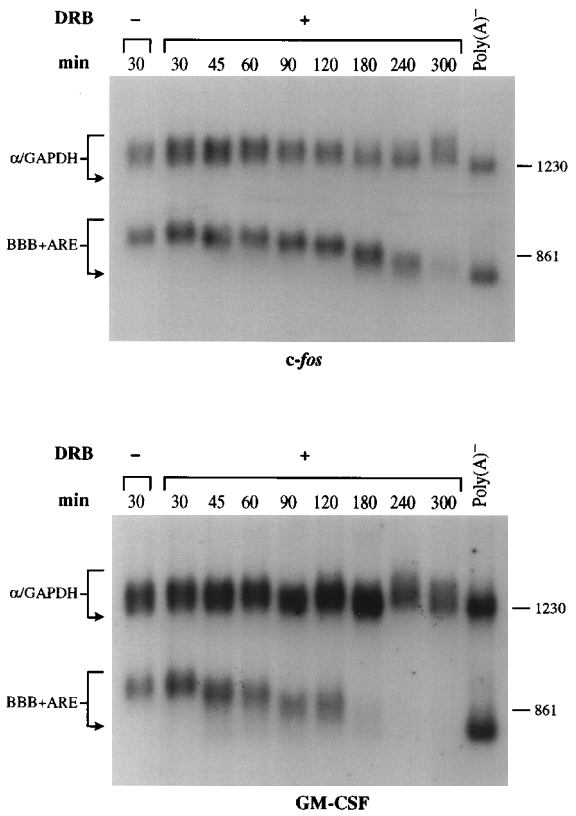

FIG. 8. Treatment of NIH 3T3 cells with transcription inhibitor DRB slowed down the decay of β-globin mRNA carrying either the c-*fos* or GM-CSF ARE. Transient cotransfection of NIH 3T3 cells with control plasmid pSVα1/GAPDH and one of the test plasmids and subsequent analysis of mRNA decay were carried out as described in the legend to Fig. 2. The times given at the top correspond to minutes after serum stimulation. DRB (20 μg/ml) was added to the culture medium 25 min after serum induction. The 30-min time point sample without (−) DRB treatment is shown as well. Poly(A)$^-$ RNA was prepared in vitro by treating RNA samples from the 30-min time point with oligo(dT) and RNase H. A 123-bp DNA ladder from BRL was used as the molecular size standard. The positions corresponding to 861 and 1,230 nt are indicated on the right.

teration in the deadenylation step of β-globin mRNA carrying the c-*fos* ARE but not the GM-CSF ARE is observed when translation initiation is inhibited by hairpin insertion. Interestingly, the change is from a fairly synchronous pattern to an asynchronous pattern. One possibility is that two pathways exist for c-*fos*-ARE-directed decay. Depending on the translation status, the mRNA may be targeted for rapid degradation by one pathway or the other. Alternatively, the translation status of an ARE-containing mRNA may affect the processivity of the RNase responsible for degrading the poly(A) tail. Finally, both ActD and DRB appear to have more profound inhibitory effects on the destabilizing function of the c-*fos* ARE than on that of the GM-CSF ARE. It is worth noting that ActD also changes the deadenylation kinetics directed by the GM-CSF ARE from rapid and asynchronous to somewhat slow and synchronous poly(A) shortening. This could be due to competitive interference by ActD in the formation of a proper ARE-protein complex that is responsible for directing rapid and asynchronous deadenylation. Taken together, these observations argue that the two AREs are targets of two distinct degradation pathways that converge on deadenylation as a critical first step. In addition, they also support our hypothesis of the existence of different classes of AREs (8) and argue that the different sequence features noted for the two classes of AUUUA-containing AREs represent a bona fide distinction that may ultimately lead to the different responses described above.

Studies of a yeast poly(A)-binding-protein-dependent poly(A) nuclease (PAN1) may shed some light on the enzymatic aspects of the in vivo deadenylation reactions mediated by the c-*fos* and GM-CSF AREs (16, 19). In particular, the two kinetically distinct deadenylation reactions described above have some similarities with the deadenylation reactions observed in vitro for yeast PAN1 (16). First, PAN1 normally shortens mRNA poly(A) tails by a slow distributive mechanism, but RNA-destabilizing elements within the mRNA can accelerate this shortening process. This is analogous to the two ARE-mediated rapid deadenylation steps. Second, PAN1 can be switched from a nonprocessive or distributive enzyme to a more processive enzyme. This is analogous to the highly processive enzymatic action associated with GM-CSF-ARE-mediated poly(A) shortening. Third, two intermediates can be found in PAN1-catalyzed deadenylation reactions in vivo. One is the poly(A)-shortened mRNA species with 10 to 25 nt of poly(A) tail derived from the distributive action of PAN1, which is analogous to the poly(A)-shortened intermediate in the c-*fos* ARE pathway. The other is the poly(A)$^-$ RNA that results from the processive action of PAN1, which is analogous to that of the GM-CSF ARE pathway. Taken together with our findings, these observations suggest that in mammalian cells, an RNase(s) analogous to yeast PAN1 exists to catalyze the kinetically distinct deadenylation reactions directed by these two AREs.

One critical but controversial issue pertaining to the destabilizing function of the ARE is whether ARE-directed mRNA decay has to be coupled to protein translation. Several recent studies showed that the GM-CSF ARE functions as an RNA-destabilizing element only when the mRNA bearing it is translated by ribosomes (1, 20), whereas the mRNA carrying the c-*fos* ARE remains unstable even when its translation is specifically inhibited (12). Our direct comparison data clearly show that both AREs retain their full destabilizing abilities when translation initiation of the mRNAs bearing them is blocked. Thus, we have demonstrated that the destabilizing functions of these two AREs can be uncoupled from ongoing translation by ribosomes. This conclusion is supported by several control experiments. First, our polysome profile studies have shown an efficient blockade of translation initiation by hairpin insertions in the tested mRNAs (Fig. 6). Second, the efficacy of targeted translation inhibition by hairpin insertion has been further demonstrated by specific stabilization of BFB mRNA carrying the same hairpin insertion (Fig. 4A). Third, we have shown that hairpin insertion per se has no destabilizing effect on stable β-globin mRNA (Fig. 4B), thus the lability of BBB-hp mRNA bearing either ARE is indeed due to the destabilizing activities of AREs. A few alternate interpretations can be proposed to explain the discrepancies between our conclusions and those of others (1, 20) concerning translation coupling of GM-CSF ARE function. One possibility is that in NIH 3T3 cells, serum induction leads to activation of an alternative pathway (see above) that is independent of the translation status of the message carrying the GM-CSF ARE. Another possibility is that there is a cell-specific factor in NIH 3T3 cells but not in the cells used in the other studies that is necessary for the GM-CSF ARE to exert a translation-independent RNA destabilization effect.

After our manuscript was submitted, Winstall et al. (27) reported that rapid mRNA degradation mediated by the c-*fos* and GM-CSF AREs occurs through similar polysome-associ-

ated mechanisms in growing NIH 3T3 cells. There is an apparent discrepancy between their conclusion and ours. One interpretation that may reconcile these seemingly contradictory results is that both AREs may require translation to function in growing cells but not in the G_0-to-G_1 transition when quiescent cells are stimulated by serum. While this issue requires further experiments for clarification, we notice that the data presented by Winstall et al. (27) may have been misinterpreted by them. They claim that the addition of hemin to iron-depleted cells induced the redistribution of ARE-containing mRNAs from nonpolysomes to polysomes, but their results show that under this translation-permissive condition, at least 60% of ARE-containing mRNAs (likely over 70% after normalization to the control message) were not associated with polysomes. However, these untranslated mRNAs were still quickly degraded. If the decay of c-*fos*- and GM-CSF-ARE-containing mRNAs is coupled to translation and can only occur to polysome-associated mRNAs as they claim, then these nonpolysome and untranslated mRNAs should have remained stable. Therefore, their data are consistent with what we report here, i.e., rapid mRNA decay mediated by two distinct AREs from c-*fos* and GM-CSF transcripts can be uncoupled from translation by ribosomes.

Two relevant observations are also worthy of discussion. When translation initiation of wild-type β-globin mRNA is blocked by hairpin insertion, not only is there no change in mRNA stability but there is also no alteration in the synchronous deadenylation process (Fig. 4, bottom panel). We propose that deadenylation of the stable β-globin mRNA is a manifestation of the cytoplasmic default mechanism of poly(A) shortening (24). If so, our data suggest that default cytoplasmic deadenylation is a translation-independent process which can be modulated or accelerated by RNA stability determinants, such as AREs and the c-*fos* protein coding region (see below). The other relevant issue concerns the destabilizing function of the c-*fos* protein coding region. Previously, we have shown that the c-*fos* protein coding region, like the c-*fos* ARE, directs biphasic decay, in which rapid and synchronous poly(A) shortening is followed by a rapid decay of the RNA body (21, 25). It is clear from our results (Fig. 4, top panel) that the c-*fos* protein coding region loses its destabilizing function when translation initiation of the mRNA bearing it (BFB mRNA) is inhibited. Interestingly, the first step in accelerated poly(A) shortening is also blocked, and BFB-hp mRNA undergoes a deadenylation indistinguishable from the default mechanism illustrated by β-globin mRNA. Therefore, unlike the situation for c-*fos* ARE, ongoing translation is necessary for the c-*fos* protein coding region to direct rapid mRNA decay through deadenylation. Thus, c-*fos* mRNA carries two structurally and functionally distinct RNA-destabilizing elements that display differential requirements for translation to exert destabilization function. Moreover, these results illustrate the importance of modulating deadenylation by various destabilizing elements as a pivotal step in mammalian mRNA decay.

On the basis of the data presented here, we propose a general model for ARE-mediated mRNA degradation in which accelerated deadenylation is a common initial step (Fig. 9A). However, rapid poly(A) shortening of the mRNA population can proceed either way: synchronous shortening due to the distributive or nonprocessive enzymatic action of an RNase, as illustrated by the c-*fos* ARE, or asynchronous shortening caused by the processive enzymatic digestion of the same or a different RNase, as illustrated by the GM-CSF ARE. These two distinct kinetics of deadenylation then lead to the production of two different mRNA intermediates. In the c-*fos* ARE pathway, the mRNA intermediate has a shortened poly(A) tail of 30 to 60 nt (6), whereas in the GM-CSF ARE pathway, the RNA intermediate has lost its poly(A) tail completely. The identification of the distinct natures of these two intermediates raises the question of whether their subsequent decay is carried out through the same exo- or endonuclease pathway. Differences in the organization of some sequence features, such as the AUUUA pentanucleotide, multiple reiterations of the AUUU tetranucleotide, and U-rich region (7, 8, 14, 29), could result in the formation of different RNA-protein complexes or different ways of organizing the same *trans*-acting factors. Consistent with this speculation are the observations that a 20S messenger RNP (mRNP) complex is specifically formed on mRNA bearing the GM-CSF ARE (20) and that there are factors which display different binding affinities for these two AREs (4). Depending on the ARE, once organized, the mRNP complex could directly influence and modulate the processivity of an RNase or recruit kinetically distinct RNases, or they could influence the stability of the poly(A) tail–poly(A)-binding-protein complex, which in turn would make poly(A) tails more susceptible to RNase attack (3). After the deadenylation step, the mRNA body could be degraded by exonuclease or endonuclease. Further work on identifying and characterizing the cognate ARE mRNP complexes and the mammalian cytoplasmic RNase(s) for degrading poly(A) tails will help elucidate these mechanisms.

It is striking that two commonly used transcription inhibitors, ActD and DRB, can lead to dramatic and specific stabilization of β-globin mRNA bearing the c-*fos* or GM-CSF ARE. The effect is particularly profound and fast when ActD is used (Fig. 7). Complete stabilization was achieved only 10 min after ActD treatment at the 25-min time point at a concentration of 5 μg/ml. The two BBB+ARE mRNAs remain stable even 20 h after ActD treatment. The observation that α/GAPDH mRNA is completely degraded during the time course experiment indicates that the inhibitory effect of ActD is somewhat ARE specific. This notion is further augmented by our previous observation that the destabilizing function of the instability determinant in the c-*fos* coding region is not affected even when 10 μg of ActD per ml is used (26). Thus, it is clear from our studies that neither the c-*fos* ARE nor the GM-CSF ARE is able to fully exert its RNA-destabilizing function when NIH 3T3 cells are treated with either transcription inhibitor after serum induction. An important lesson to be learned from our study is that investigations of mRNA stability with transcription inhibitors must be interpreted with extreme care, especially in the case of ARE-mediated decay.

A critical issue remaining to be addressed is how these nuclear transcription inhibitors may function to inhibit mRNA decay in the cytoplasm. A few recent studies showed that after the treatment of cells with ActD or DRB for 3 h, a significant two- to threefold accumulation of a U-rich-sequence-binding protein (URBP), termed AU-A, as well as hnRNP A1 protein, in the cytoplasm was observed (11, 17). Interestingly, both AU-A and hnRNP A1 proteins have also been shown to bind to the c-*fos* and GM-CSF AREs in in vitro studies (9, 11). In addition, several other ARE-binding proteins with high affinities to U-rich sequences are also found in both the cytoplasm and the nucleus (5, 11); we have called them URBPs (28). One speculative model explains how ActD and DRB function to block ARE-mediated mRNA decay (Fig. 9B). After the arrest of nuclear transcription by ActD or DRB, certain hnRNP and probably some other URBPs might be transported from the nucleus to the cytoplasm by various means. For example, they might be transported to the cytoplasm in a free form released from nuclear RNA degradation or along with mature mRNAs in a form of mRNP complex (17). This might lead to a tem-

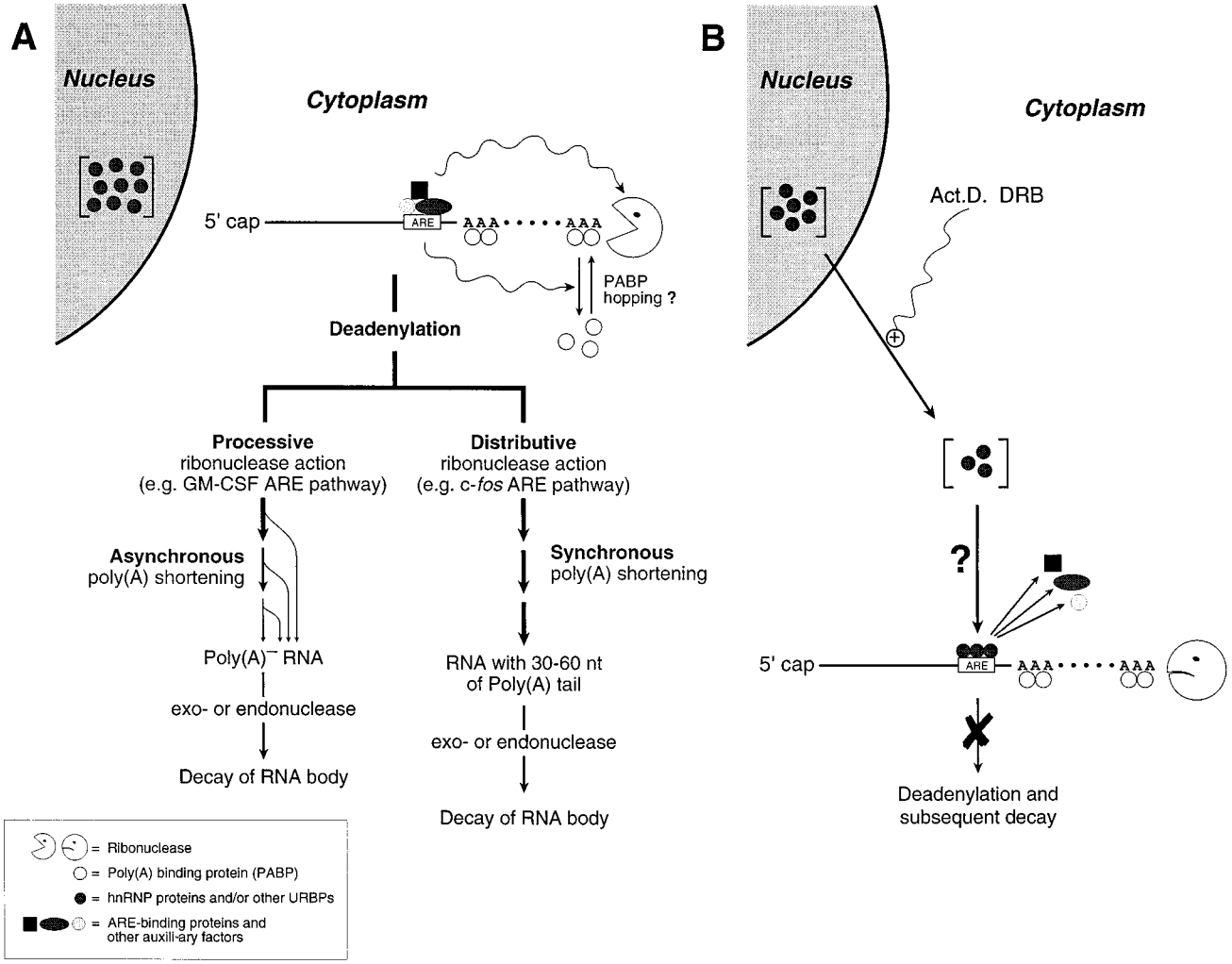

FIG. 9. (A) General model for ARE-mediated mRNA degradation showing the two distinct deadenylation pathways represented by c-*fos* and GM-CSF AREs. (B) Model for the effects of ActD and DRB on the destabilizing functions of AREs. See text for the details.

porary increase in the cytoplasmic levels of these proteins, which could in turn result in displacement of the binding of authentic cognate ARE-binding proteins in the cytoplasm or alternatively in a change of the cytoplasmic equilibrium of binding between these proteins and AREs. As a result, this might lead to disruption of the functional ARE-protein complex necessary for ARE-directed mRNA decay. Thus, the inhibition of transcription could lead to mRNA stabilization. It is noteworthy that the differential inhibitory effects of ActD and DRB on ARE-mediated mRNA decay are consistent with the extents of overall transcription inhibition achieved by the two drugs, e.g., over 99% inhibition by ActD (5 μg/ml) and 60% inhibition by DRB (20 μg/ml) in NIH 3T3 cells (unpublished data). Therefore, it is possible that the greater the inhibition a drug can achieve, the more nuclear hnRNP and URBPs can be released to the cytoplasm. The extent of the mRNA stabilization effect may differ among various AREs, depending on their affinities for these proteins.

In summary, AREs appear to direct selective mRNA decay through a rather intricate process. Our finding of distinct pathways for deadenylation provides an important new insight into the mechanism and regulation of the ARE-directed decay pathway. The two distinct ways for facilitating deadenylation by the c-*fos* and GM-CSF AREs may have a general implication for eukaryotic mRNA degradation in that deadenylation is a critical first step in the decay of many mRNAs in both yeast and mammalian cells.

ACKNOWLEDGMENTS

We thank Jack A. DeMoss and Julia Lever for critical reading of the manuscript and valuable comments, Paul Gershon and Jeff Ross for helpful discussions, Jose Garcia-Sanz for assistance in polysome profile studies, Marilyn Kozak for providing the hairpin plasmid, and Beto Zúñiga for expert photography and artwork.

This work was supported by NIH grant GM-46454 and an American Cancer Society Junior Faculty Research award (to A.-B.S.). A.-B.S. is the recipient of an American Heart Association Established Investigator Award. C.-Y.A.C. is the recipient of a research planning award from the National Science Foundation.

REFERENCES

1. **Aharon, T., and R. J. Schneider.** 1993. Selective destabilization of short-lived mRNAs with the granulocyte-macrophage colony-stimulating factor AU-rich 3′ noncoding region is mediated by a cotranslational mechanism. Mol. Cell. Biol. **13:**1971–1980.
2. **Beelman, C. A., and R. Parker.** 1995. Degradation of mRNA in eukaryotes. Cell **81:**179–183.
3. **Bernstein, P., S. W. Peltz, and J. Ross.** 1989. The poly(A)-poly(A)-binding

protein complex is a major determinant of mRNA stability in vitro. Mol. Cell. Biol. **9:**659–670.
4. **Bohjanen, P. R., B. Petryniak, C. H. June, C. B. Thompson, and T. Lindsten.** 1991. An inducible cytoplasmic factor (AU-B) binds selectively to AUUUA multimers in the 3′ untranslated region of lymphokine mRNA. Mol. Cell. Biol. **11:**3288–3295.
5. **Burd, C. G., and G. Dreyfuss.** 1994. Conserved structures and diversity of functions of RNA-binding proteins. Science **265:**615–621.
6. **Caput, D., B. Beutler, K. Hartog, R. Thayer, S. Brown-Shimer, and A. Cerami.** 1986. Identification of a common nucleotide sequence in the 3′-untranslated regions of mRNA molecules specifying inflammatory mediators. Proc. Natl. Acad. Sci. USA **83:**1670–1674.
7. **Chen, C.-Y. A., T.-M. Chen, and A.-B. Shyu.** 1994. Interplay of two functionally and structurally distinct domains of the c-*fos* AU-rich element specifies its mRNA-destabilizing function. Mol. Cell. Biol. **14:**416–426.
8. **Chen, C.-Y. A., and A.-B. Shyu.** 1994. Selective degradation of early-response-gene mRNAs: functional analyses of sequence features of the AU-rich elements. Mol. Cell. Biol. **14:**8471–8482.
9. **Hamilton, B. J., E. Nagy, J. S. Malter, B. A. Arrick, and W. F. C. Rigby.** 1993. Association of heterogeneous nuclear ribonucleoprotein A1 and C proteins with reiterated AUUUA sequences. J. Biol. Chem. **268:**8881–8887.
10. **Higuchi, R.** 1990. Recombinant PCR, p. 177–183. *In* M. A. Innis, D. H. Gelfand, J. J. Sninsky, and T. J. White (ed.), PCR protocols: a guide to methods and applications. Academic Press, San Diego, Calif.
11. **Katz, D. A., N. G. Theodorakis, D. W. Cleveland, T. Lindsten, and C. B. Thompson.** 1994. AU-A, an RNA-binding activity distinct from hnRNP A1, is selective for AUUUA repeats and shuttles between the nucleus and the cytoplasm. Nucleic Acids Res. **22:**238–246.
12. **Koeller, D. M., J. A. Horowitz, J. L. Casey, R. D. Klausner, and J. B. Harford.** 1991. Translation and the stability of mRNAs encoding the transferrin receptor and c-*fos*. Proc. Natl. Acad. Sci. USA **88:**7778–7782.
13. **Kozak, M.** 1989. Circumstances and mechanisms of inhibition of translation by secondary structure in eucaryotic mRNAs. Mol. Cell. Biol. **9:**5134–5142.
14. **Lagnado, C. A., C. Y. Brown, and G. J. Goodall.** 1994. AUUUA is not sufficient to promote poly(A) shortening and degradation of an mRNA: the functional sequence within AU-rich elements may be UUAUUUA(U/A)(U/A). Mol. Cell. Biol. **14:**7984–7995.
15. **Lindsten, T., C. H. June, J. A. Ledbetter, G. Stella, and C. B. Thompson.** 1989. Regulation of lymphokine messenger RNA stability by a surface-mediated T cell activation pathway. Science **244:**339–343.
16. **Lowell, J. E., D. R. Rudner, and A. B. Sachs.** 1992. 3′-UTR-dependent deadenylation by the yeast poly(A) nuclease. Genes Dev. **6:**2088–2099.
17. **Piñol-Roma, S., and G. Dreyfuss.** 1992. Shuttling of pre-mRNA binding proteins between nucleus and cytoplasm. Nature (London) **355:**730–732.
18. **Ross, J.** 1995. mRNA stability in mammalian cells. Microbiol. Rev. **59:**16–95.
19. **Sachs, A. B.** 1993. Messenger RNA degradation in eukaryotes. Cell **74:**413–421.
20. **Savant-Bhonsale, S., and D. W. Cleveland.** 1992. Evidence for instability of mRNAs containing AUUUA motifs mediated through translation-dependent assembly of a >20S degradation complex. Genes Dev. **6:**1927–1939.
21. **Schiavi, S. C., C. L. Wellington, A.-B. Shyu, C.-Y. A. Chen, M. E. Greenberg, and J. G. Belasco.** 1994. Multiple elements in the c-*fos* protein-coding region facilitate deadenylation and decay by a mechanism coupled to translation. J. Biol. Chem. **269:**3441–3448.
22. **Schuler, G. D., and M. D. Cole.** 1988. GM-CSF and oncogene mRNA stabilities are independently regulated in trans in a mouse monocytic tumor. Cell **55:**1115–1122.
23. **Shaw, G., and R. Kamen.** 1986. A conserved AU sequence from the 3′ untranslated region of GM-CSF mRNA mediates selective mRNA degradation. Cell **46:**659–667.
24. **Sheiness, D., and J. E. Darnell.** 1973. Polyadenylic acid segment in mRNA becomes shorter with age. Nature (London) **241:**265–268.
25. **Shyu, A.-B., J. G. Belasco, and M. E. Greenberg.** 1991. Two distinct destabilizing elements in the c-*fos* message trigger deadenylation as a first step in rapid mRNA decay. Genes Dev. **5:**221–231.
26. **Shyu, A.-B., M. E. Greenberg, and J. G. Belasco.** 1989. The c-*fos* transcript is targeted for rapid decay by two distinct mRNA degradation pathways. Genes Dev. **3:**60–72.
27. **Winstall, E., M. Gamache, and V. Raymond.** 1995. Rapid mRNA degradation mediated by the c-*fos* 3′ AU-rich element and that mediated by the granulocyte-macrophage colony-stimulating factor 3′ AU-rich element occur through similar polysome-associated mechanisms. Mol. Cell. Biol. **15:**3796–3804.
28. **You, Y., C.-Y. A. Chen, and A.-B. Shyu.** 1992. U-rich sequence-binding proteins (URBPs) interacting with a 20-nucleotide U-rich sequence in the 3′ untranslated region of c-*fos* mRNA may be involved in the first step of c-*fos* mRNA degradation. Mol. Cell. Biol. **12:**2931–2940.
29. **Zubiaga, A. M., J. G. Belasco, and M. E. Greenberg.** 1995. The nonamer UUAUUUAUU is the key AU-rich sequence motif that mediates mRNA degradation. Mol. Cell. Biol. **15:**2219–2230.